THE MADISON SYMMETRIC TORUS

EXPERIMENTAL DEVICES

KEYWORDS: *reversed-field pinch, magnetics, plasma confinement*

R. N. DEXTER, D. W. KERST, T. W. LOVELL, S. C. PRAGER, and J. C. SPROTT *University of Wisconsin, Department of Physics 1150 University Avenue, Madison, Wisconsin 53706*

Received November 13, 1989
Accepted for Publication April 26, 1990

The Madison Symmetric Torus (MST) is the newest and largest reversed-field pinch (RFP) currently in operation. It incorporates a number of design features that set it apart from other pinches, including the use of the conducting shell as both a vacuum vessel and single-turn toroidal field coil. Specially insulated voltage gaps are exposed to the plasma. Magnetic field errors at these gaps as well as at the various diagnostic and pumping ports are minimized through a variety of techniques. The physics goals of MST include study of the effect of large plasma size on confinement and the detailed investigation of RFP turbulence, dynamo, and transport. Details of the design and initial operation of the device are presented.

I. INTRODUCTION

The Madison Symmetric Torus (MST) is a toroidal reversed-field pinch (RFP) device for plasma physics and fusion research. After a 3-yr construction period, the first plasma operation began in June 1988. The MST is a large RFP with a minor radius of 0.52 m and a major radius of 1.5 m. Although similar in size to the two "next-generation" RFP experiments (RFX at the National Research Council in Padua, Italy,[1] and ZTH at the Los Alamos National Laboratory[2]), MST has a much lower volt-second capability and consequent lower plasma current (<1 MA compared to 2 to 4 MA) and discharge duration (~40 ms compared to several hundred milliseconds). These limitations arise from the use of an iron-core transformer and a thick conducting shell to provide the equilibrium fields, and they do not compromise the objectives of the device, which are to study basic physics issues of toroidally confined plasmas.

Since the minor radius is about twice that of the next largest currently operating RFP, the prediction of the plasma parameters is less certain, and their characterization has constituted one of the first experimental tasks. This paper describes the major design features of the facility and shows experimental waveforms from its initial operation.

The two main goals of the MST experiment are (a) to investigate the effect of large plasma size on RFP confinement, particularly on parameters such as plasma beta and energy confinement time, and (b) to study turbulence (magnetic and electrostatic), dynamo, and transport.

Three criteria heavily influenced the design of MST. First, it was required, as is true for all new RFP experiments, that the magnetic field errors due to the shell, gaps, port holes, and field windings be minimized. To investigate the innate turbulence and transport, it is crucial to minimize the extraneous effects of magnetic field errors. There is ample evidence from other RFP experiments of the influence of field errors on plasma behavior.[3-6] Second, good diagnostic access is desirable, as is necessary for optimal resolution of fluctuations and transport. Third, expeditious disassembly is necessary in order to alter the boundary and internal diagnostics. Alteration of the boundary (such as limiters or wall coatings) might be necessary to minimize the extraneous effects of plasma/wall interactions. In addition, the machine can be used to investigate the required electrical boundary condition (the problem of the stabilizing shell) by inserting within the vacuum vessel toroidal shells of smaller minor radii (on the order of 30 cm) with variable wall thickness or spatial structure.

The machine design that resulted from these considerations employs unique features in the poloidal field (PF), toroidal field (TF), and vacuum pumping systems. Illustrative views of the machine are presented in Figs. 1 and 2. All the windings that constitute the PF system are wrapped tightly around the iron core and do

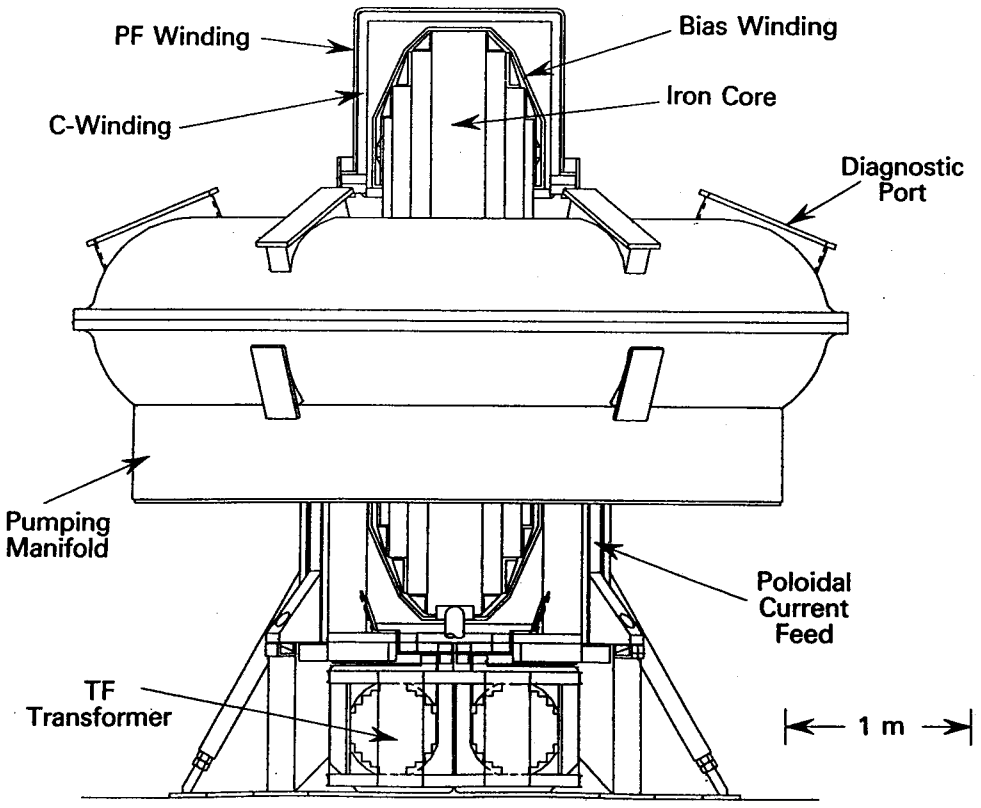

Fig. 1. Overview of the MST device.

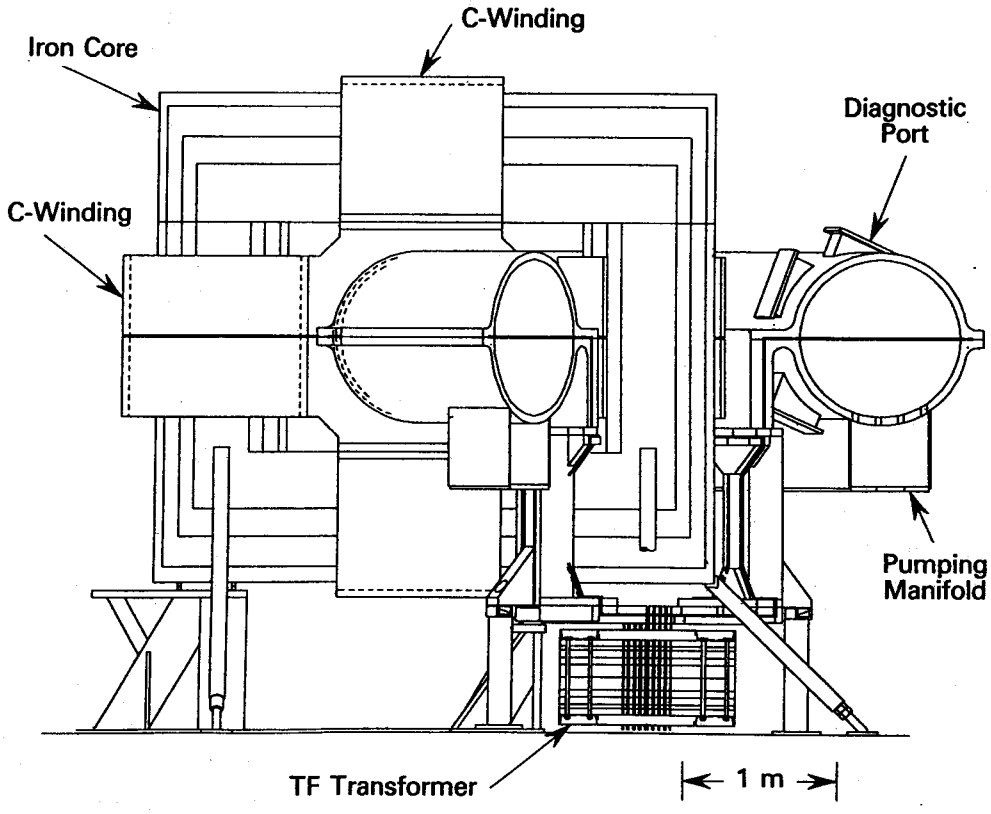

Fig. 2. Cutaway of the MST device.

not axisymmetrically encircle the toroid. The toroidal field is produced by driving current through the aluminum shell. Hence, the machine is totally unencumbered with field coils, which is advantageous for disassembly and diagnostic access.

To maintain a small value of error field at the poloidal gap (the vertical cut in the shell that allows the poloidal magnetic field to enter) requires two separate sets of windings around the core: the PF winding, which is distributed so as to match the plasma image currents flowing on the inside wall of the torus, and the continuity winding (C-winding) or jacket, which carries the wall current from one side of the gap, around the core, to the other side. At the gap, the torus is connected to the C-winding by an extended flange that reduces errors due to improper distribution of the PF winding. A third winding surrounds the core to provide the reverse bias and is distributed for minimal dc flux leakage.

The use of the vacuum vessel, with an extended flange connection, as the TF winding produces a toroidal field with negligible ripple. The error due to port holes is kept small by pumping the vacuum through one hundred ninety-three 3.8-cm-diam holes rather than through a smaller number of large perturbing holes. The various systems have been designed so that the residual field errors produce magnetic islands within the plasma that cover <10% of the minor radius in total and that produce field distortions at the plasma surface of <1 cm. Satisfaction of these criteria requires calculation of the spatial Fourier composition of the error, which differs from case to case.

The use of the shell as vacuum vessel eliminates the problem of plasma damage to the thin vacuum liners used in other devices, but at the expense of requiring voltage gaps that are exposed to the plasma, leading to the possibility of arcing. The insulation problem has been solved by gap protectors developed and tested in previous RFP experiments at the University of Wisconsin.[7] No arcing damage occurred in 3 yr of operating with the final design, including 1 yr in MST. Plasma is prevented from reaching the actual gap insulator, a Viton 6-mm-thick strip, which also serves as the shell vacuum gasket, as shown in Fig. 3. The metal near the actual gap has gently rounded edges; closely fitted machinable ceramic forms cover all voltage insulators and extend 1 cm into the plasma over their 10-cm width. Below is a brief description of the major subsystems, including the vacuum vessel and pumping system (Sec. II), the PF system (Sec. III), and the TF system (Sec. IV). The projected plasma parameters are described in Sec. V, and waveforms from initial operation are included in Sec. VI.

II. VACUUM VESSEL AND PUMPING

The vacuum vessel serves the three functions of vacuum containment, TF winding, and shell for plasma equilibrium and stability. It is interchangeably referred to as the shell or vacuum vessel. The MST will initially be operated without vertical field (VF) coils, since the outer magnetic surface is extremely close to the shell, whose time constant exceeds the pulse length. Space outside the vessel is reserved for VF coils if they are later deemed necessary. The vacuum vessel, shown in Fig. 4, is made from 5-cm-thick 6061-T6 aluminum and has a minor radius of 0.52 m and a major radius of 1.5 m. The vessel is split at the midplane into two halves, which are bolted together. The outer bolted joint is an electrical contact treated with Alcoa Electrical Joint Compound on the air side of the joint. An insulated, 1.3-cm-wide "toroidal gap" (for entry of the toroidal magnetic field) resides on the side of the small major radius. Welded to the vessel at this gap are disk flanges that carry the current to produce the toroidal field. The vessel is sealed, both toroidally and poloidally, with flat Viton gaskets. The poloidal and toroidal seals meet at two intersections, referred to as the triple joints. The poloidal gap is 1.3 cm wide and is welded to the poloidal flange, which then connects to the continuity winding.

Vacuum pumping is through an array of 193 small holes with a hole-to-hole spacing of ~15 cm or four hole diameters. The array is situated on the bottom of the vessel and extends 270 deg in the toroidal direction. A pumping manifold that encloses the hole array is welded to the vessel (as shown in Figs. 1, 2, and 4). The hole separation is sufficiently large that the wall

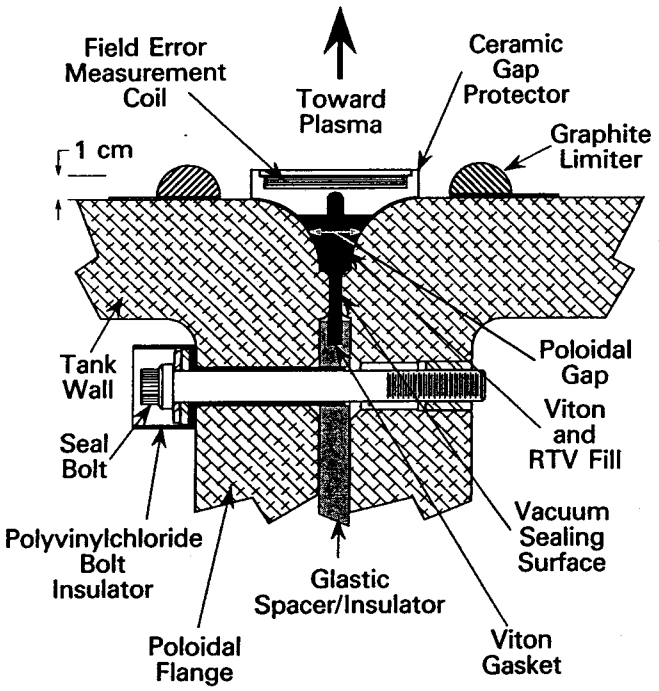

Fig. 3. Gap protection, insulation, and vacuum sealing configuration.

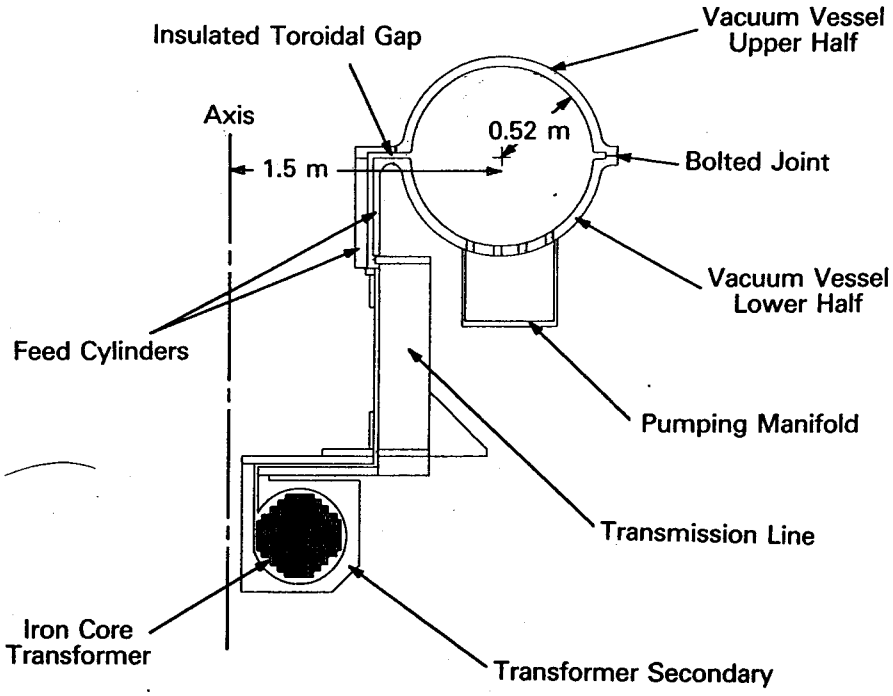

Fig. 4. MST vacuum vessel, pumping duct, and TF system.

current distortion produced by the holes are noninterfering. Thus, the holes produce only small field perturbations that are localized to the vicinity of the holes. Toroidal axisymmetry is preserved by the use of additional dummy holes that do not completely penetrate the shell over the 90-deg segment without a pumping manifold. The vessel is equipped with 175 diagnostic ports of 5-cm diameter or smaller and four 11.4-cm-diam ports (which form two intersecting tangential lines of sight).

The bottom of the pumping manifold contains seventeen 18.6-cm-diam pumping holes, which do not affect the magnetic field within the vessel. The 193 small holes allow a maximum pumping speed (for nitrogen) of 22 000 ℓ/s. Initially, four turbomolecular pumps and a cryopump are being used, but gettering within the manifold will be added later to enlarge the options for vacuum and impurity control.

III. PF SYSTEM

The major components of the system that produces the poloidal magnetic field and toroidal plasma current are the C-winding and poloidal flange, the PF winding, and the bias winding. Each component is described below.

III.A. C-Winding and Poloidal Flange

The C-winding is a feature necessary to avoid a large error at the poloidal gap in machines with field windings wrapped around the iron core, as opposed to the usual axisymmetric windings. The C-winding concept is illustrated in Fig. 5. The C-winding is a conducting sheet that is connected across the poloidal gap by a path that surrounds, but does not link, the iron core. The wall current that flows on the plasma side of the shell (which is an image of the plasma current) on reaching the gap continues through the flanges and C-winding to the other side of the gap. Without the C-winding, the current would transfer to the outside surface of the shell at the gap. Since the outside current distribution would differ from that on the inner surface, a poloidal component to the current would exist along the gap edge to connect the two distributions, thereby producing an error magnetic field in the direction of the minor radius. The distribution of current in the C-winding is the imposed image of the nearby PF winding, which is distributed at the flange to match the internal wall current distribution.

As depicted in Fig. 5, the C-winding is connected to the gap through a poloidal flange, shown in Fig. 6. The inner circular surface of the aluminum flange is welded to the shell. The outer surface is roughly rectangular and is connected to the four sections of the C-winding, each of which surrounds one leg of the iron core (see Fig. 2). The poloidally symmetric division of the C-winding into four sections encircling the core does not significantly compromise the field error control. For the plasma current profile for which the PF placement is designed, the division of the C-winding has no detrimental effect. In this case, in which the PF

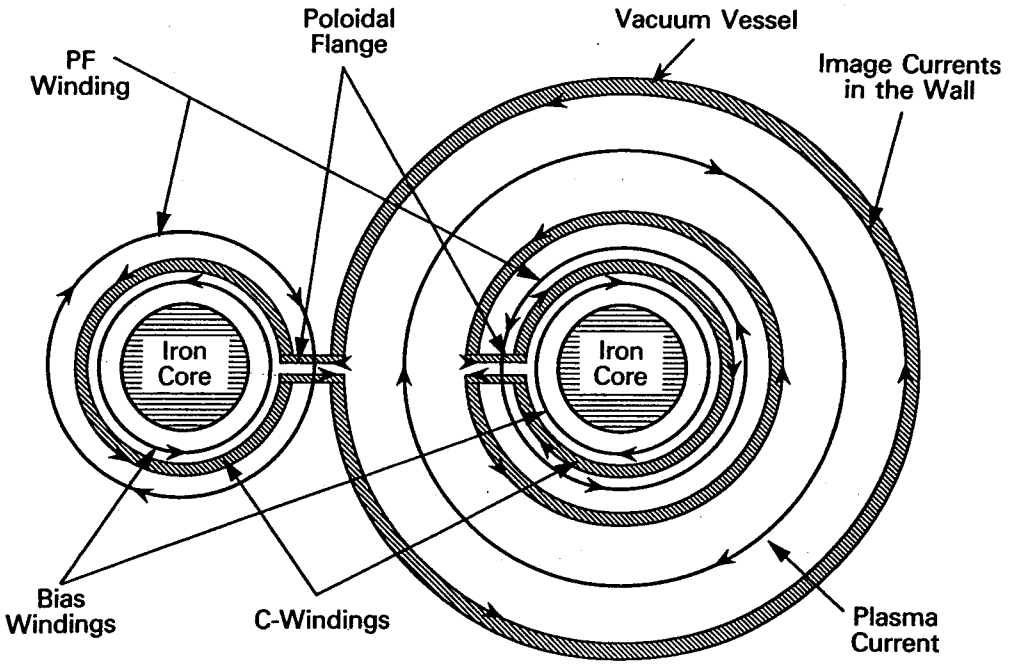

Fig. 5. MST PF system.

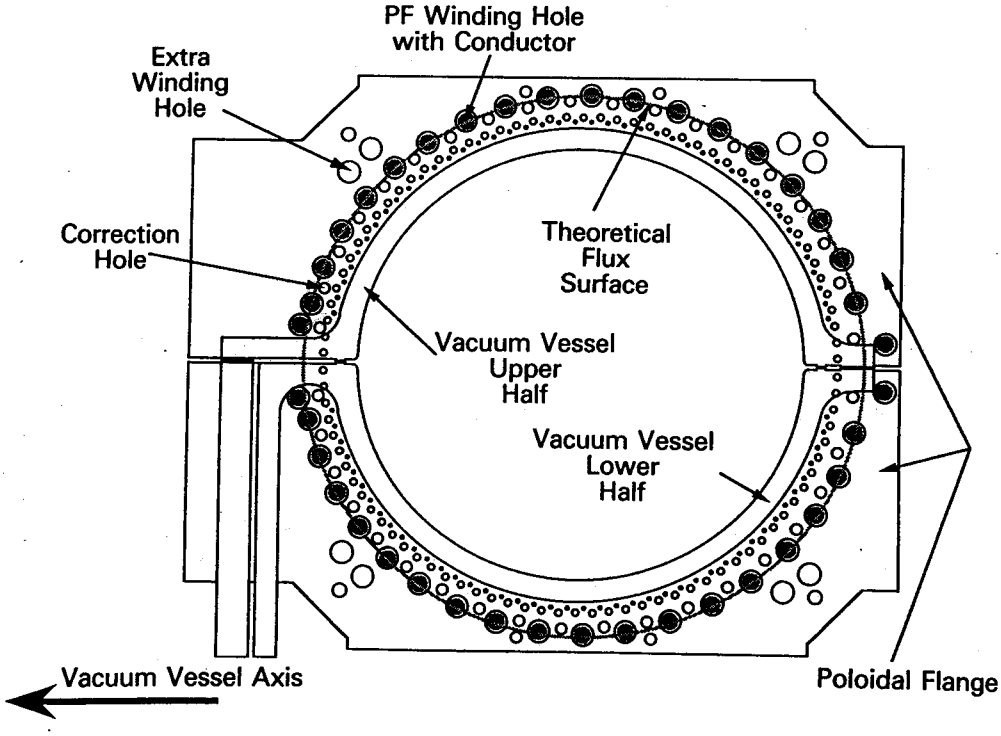

Fig. 6. MST poloidal flange.

windings lie exactly on a magnetic surface, the flange current (and hence the field error) is unaffected by the flange and C-winding poloidal shape beyond the PF winding holes. In the case in which the PF winding is mismatched to the plasma equilibrium, the finite flange size and divided C-winding limit the field error, minimizing the effect of the flange. The two side parts of the C-winding are split in half to allow lifting of the

top half of the shell with the C-winding intact. The purpose of the flange is to reduce field errors that result from improper distribution of the field windings. The flange effect arises since poloidal current resulting from winding errors need not be localized to the gap at the shell, but can flow over the entire flange, which is more distant from the plasma. As seen in Fig. 6, the flange contains numerous holes for the PF winding, field error correction coils, and field error detection coils. The flange consists of two parallel sheets of 5-cm-thick aluminum, separated by 1.25-cm-thick glastic insulator. The C-winding is 5-cm-thick aluminum, except a portion of the side winding surrounding the center leg, which was reduced to a thickness of 2.5 cm due to space limitation. For times beyond the electrical penetration time of the C-winding (~40 ms), a portion of the wall current will flow along the outside of the shell rather than through the C-winding, with an increase in field errors.

III.B. The PF Winding

The function of the PF winding is to induce the ohmic voltage and to force the current in the C-winding to flow with a poloidal distribution as required for minimal gap field error. The PF winding consists of 40 copper bars that surround the outside of the C-winding and pierce the poloidal flange through the holes depicted in Fig. 6. The current through each turn induces an equal amount of flange current to flow through the hole to the outer side of the C-winding. The total ampere-turns in the PF winding differs from the plasma current only by the small additional current required to magnetize the iron core. The desired hole placement for the turns of the winding is determined by the plasma equilibrium. A plasma magnetohydrodynamic equilibrium code has been used to calculate the shell current distribution. This distribution then serves as a boundary condition for the current entering the flange, which, through solution of equations for the flange region, determines the current everywhere on the flange. The PF winding holes are chosen to lie on a magnetic flux surface within the flange with the appropriate spacing of turns. The distribution will be imperfect for plasma current and pressure profiles that differ from those assumed in the equilibrium code. The deviation of the plasma equilibrium from the design case is expected to produce a radial magnetic field at the poloidal gap with a dominant $m = 1$ poloidal mode number and an amplitude of the order of 10% of the poloidal field.

The PF winding is in eight bundles of five turns each with separate leads, allowing numerous series and parallel combinations with turn ratios between 5:1 and 40:1. Additional holes in the poloidal flange were added to accommodate extra turns under passive or active feedback control to transpose the PF current and eliminate residual field errors. Initial correction coils will be driven by placing the coils in series with the PF winding. Feedback control will be developed only if correction fields with a time dependence different from the plasma current are required. The PF winding was installed during the summer and fall of 1989. Initial plasma operation without the PF winding employed only the bias winding to produce the ohmic voltage.

III.C. Bias Winding

The bias winding is used to reverse bias the iron core in order to accomplish a 2-Wb flux swing. This 40-turn winding consists of 4/0 welding cable potted in epoxy. A stainless steel form surrounds the core and serves as a support for the winding. The bias winding is insulated from the stainless steel form to 40 kV. The winding carries a current of up to 24 kA-turns for 3 to 10 s.

It is critical that the bias winding be distributed to minimize flux leakage into the plasma volume. Since it carries a dc current, the resultant error flux would enter the plasma through the entire shell surface, not just at the gap as for a pulsed error. Such an error is particularly damaging and difficult to correct. Thus, the desired distribution of the bias winding around the core was determined empirically. A test winding was wrapped around the bare core and repositioned using a pocket compass until the measured field was sufficiently small. The placement tests were able to reduce the stray field within the plasma region as measured with a Hall probe to a value of <1 G everywhere, as illustrated in Fig. 7.

IV. TF SYSTEM

To produce the toroidal magnetic field, poloidal current is driven around the shell as shown in Fig. 4. The current enters the shell at the insulated toroidal

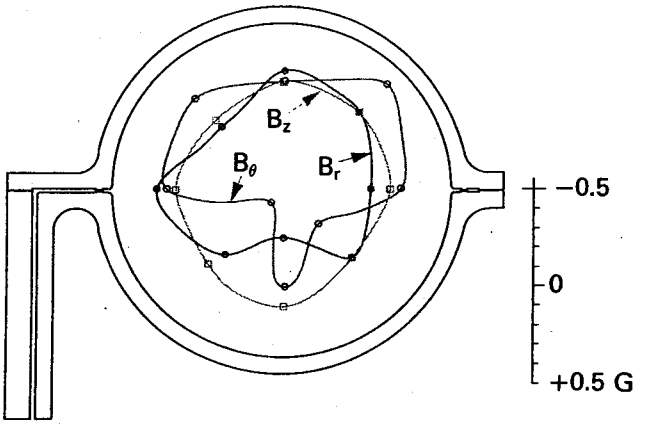

Fig. 7. Field errors due to dc bias winding, measured along a square contour that circumscribes the vacuum vessel.

gap located at the midplane on the inside of the torus. Current is fed to the shell by an axisymmetric flange system, so as to symmetrize the shell currents. The flange consists of an annular horizontal disk portion with a 15-cm radial extent that connects to a 65-cm-long cylindrical section. The transmission lines from the TF transformer connect to the bottom of the cylinders at four locations with each connection extending ~39 deg toroidally. The four transmission lines are independent secondary windings on the 0.5-Wb (full-swing) TF transformer. This transformer has four 12-turn primaries that can be connected in any combination of series and parallel. The disk flange is welded to the shell and is bolted to the cylindrical section. The dominant resonant Fourier component of the ripple in the toroidal magnetic field is $m = 0$, $n = 4$, and has an amplitude of ~0.01% on the machine minor axis. The resultant magnetic island width is ~1 cm.

Initial operation used a 450-V, 1.5-F, 152-kJ capacitor bank and required that the plasma provide the field reversal. After reversal is achieved, the 450-V bank is switched out, and a 75-V, 4.7-F, 13-kJ power crowbar bank is switched in, as shown in Fig. 8. Also available is a 5-kV, 0.015-F, 187-kJ capacitor bank that can be used to aid the reversal by allowing the TF circuit to ring backwards. The TF system was designed mechanically for a 6-kG capability so as to allow both RFP and tokamak plasmas to be produced in the same device.

V. PROJECTED PLASMA PARAMETERS

The projected plasma parameters for MST were determined by a combination of electrical circuit modeling[8] of the experimental hardware and scaling of plasma parameters with plasma current and machine size from existing devices. Since the scaling laws are generally not accurately known, a range of possibilities that presumably bracket the actual case was considered. The ultimate performance of MST is determined by the 2.0-Wb (full-swing) limit of the iron transformer core. The predicted parameters are adequate for the proposed physics research under even the most pessimistic assumptions.

The major uncertainty in the projection is the scaling of plasma resistance (or loop voltage). The pessimistic limit was obtained using the resistance achieved in the similar-sized, University of Wisconsin noncircular RFP (Ref. 7). For an optimistic prediction, the resistivity achieved in the TPE-1RM15 device[6] in Japan was used. The loop voltage in MST was thus predicted to lie in the range of 4 to 75 V. The resultant pessimistic and optimistic sets of parameters, obtained from electrical circuit modeling that includes the plasma as an element that couples the PF and TF circuits, is shown in Table I. The energy confinement times follow from the resistivity and the assumption that the poloidal beta values are 10 and 20% for the two cases, respectively. Also shown are the corresponding parameters achieved during initial operation.

VI. EXPERIMENTAL WAVEFORMS

The device was initially operated using the bias winding to drive the plasma current, with a consequent large magnetic field error at the poloidal gap. In addition, the full PF capacitor bank and waveform-shaping circuitry were not installed. Schematic representations of the PF and TF circuits used initially are shown in Fig. 8. Nevertheless, the electrical waveforms as shown in Fig. 9 agree well with the circuit modeling.

Despite the large field errors, the highest current discharges (500 kA) have a loop voltage of ~30 V, line-averaged densities (as measured by microwave interferrometry) of $\sim 1 \times 10^{19}$ m^{-3}, and electron temperatures on axis (as measured by Thomson scattering) of ~300 eV. The pinch parameter and field reversal parameter exhibit behavior similar to other RFPs. If the ion temperature is of the same order as the electron temperature and the profiles are relatively flat, one concludes that the energy confinement time is of the order of 1 ms.

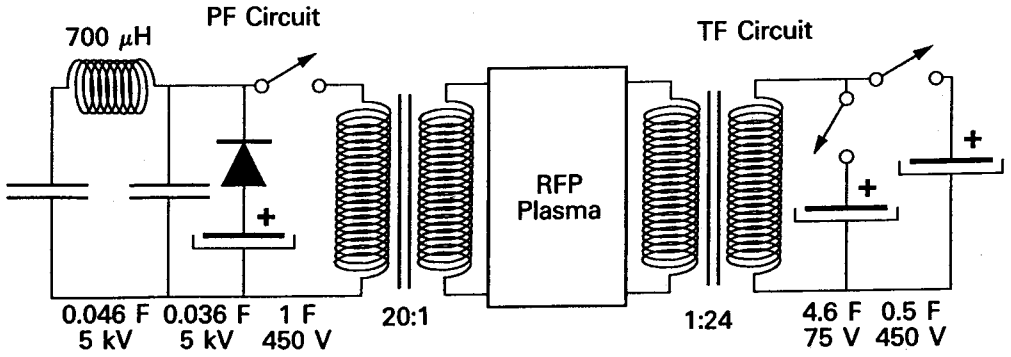

Fig. 8. Schematic representation of the PF andTF circuits.

TABLE I

Summary of Predicted and Achieved Parameters for MST

Parameter	Pessimistic	Optimistic	Achieved
Plasma current, I_p (MA)	0.4	1	0.5
Loop voltage, V_l (V)	75	4	30
Ohmic power, P_{OH} (MW)	30	4	15
Average toroidal field, $\langle B_T \rangle$ (kG)	1	2.5	1.2
Flux consumption, $\Delta\Phi$ (Wb)	1.8	1.6	1.4
Line-averaged density, $\langle n \rangle$ (m^{-3})	3×10^{19}	4×10^{19}	1×10^{19}
Central electron temperature, T_{e0} (eV)	100	1000	300
Energy confinement time, τ (ms)	0.4	10	1
Plasma duration, T (ms)	10	40	36

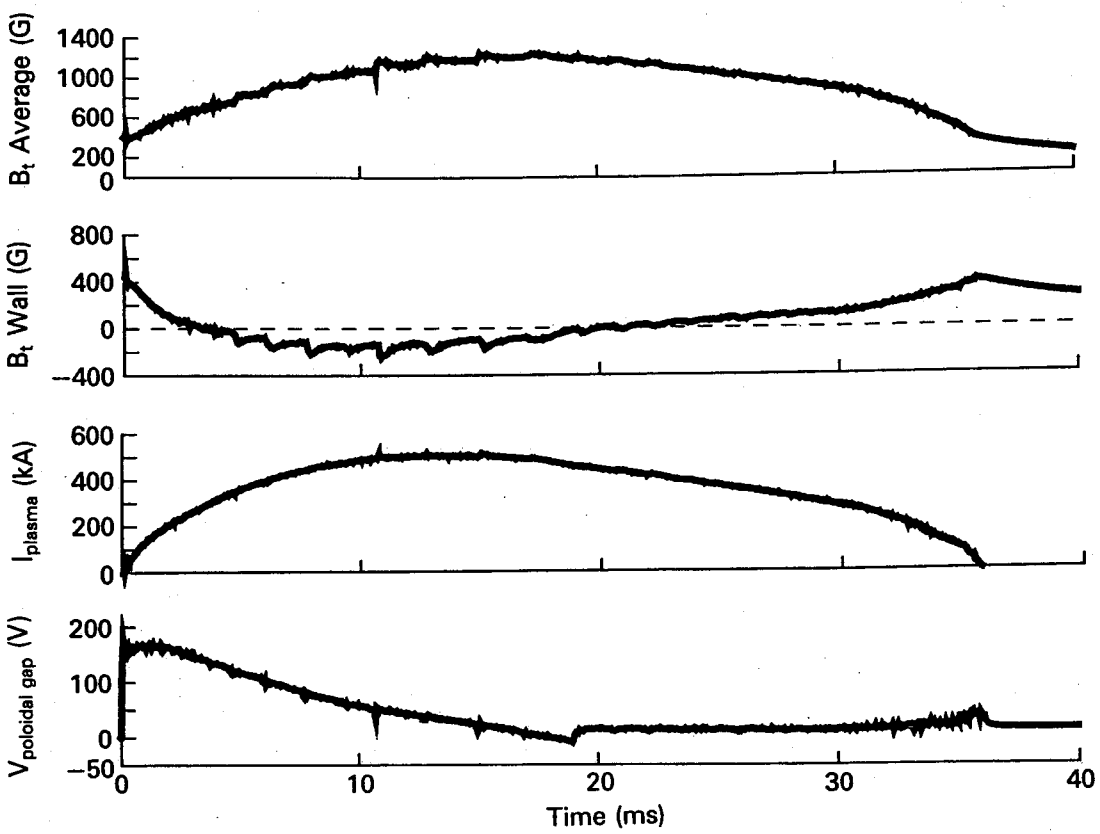

Fig. 9. Typical electrical waveforms from MST discharge.

VII. SUMMARY

The MST device has been successfully brought into operation with electrical characteristics and plasma parameters well within the range of design values. Operation has proved extremely reliable with >30 000 shots during the first year and negligible unscheduled downtime. With completion of the PF winding and upgrades of the capacitor banks and diagnostics, the device will enter its next phase of experimental operation.

ACKNOWLEDGMENTS

Much of the detailed engineering design and component fabrication was done under the direction of Farshid Feyzi at the University of Wisconsin Physical Sciences Laboratory. The vacuum vessel was constructed by Depretto-Escher-Wyss in Schio, Italy. Many aspects of the installation were supervised by John Laufenferg. Assistance with the the PF winding was provided by Ernie Newman of the Los Alamos National Laboratory.

This work was supported by the U.S. Department of Energy.

REFERENCES

1. G. MAELESANI, "The RFX Experiment," *Int. School Plasma Physics, Physics of Mirrors, Reversed Field Pinches and Compact Tori*, Varenna, Italy, September 1–11, 1987, Vol. 1, p. 331 (1987).

2. H. DREICER, "The Rationale for the Design of CPRF/ZTH, The Next Step in the U.S. RFP Program," *Int. School Plasma Physics, Physics of Mirrors, Reversed Field Pinches and Compact Tori*, Varenna, Italy, Vol. 1, p. 359 (1987).

3. K. HATTORI, K. ITAMI, T. FUJITA, J. MORIKAWA, H. NIHEI, Z. YOSHIDA, N. INOUE, H. JI, A. FUJISAWA, N. ASAKURA, K. YAMAGISHI, T. SHINOHARA, Y. NAGOYAMA, H. TOYAMA and K. MIYAMOTO, "Magnetic Field Fluctuations in Ripple Reduction Experiments on the Repute-1 RFP," *Nucl. Fusion*, **28**, 311 (1988).

4. R. B. HOWELL and H. F. VOGEL, "Magnetic Field Perturbations Due to a Hole in a Conducting Wall on the ZT-40M Reversed-Field Pinch," *J. Appl. Phys.*, **56**, 2017 (1984).

5. P. G. NOONAN, H. TSUI, and A. A. NEWTON, "Toroidal Equilibrium in the Reversed Field Pinch Corrected by a Vertical Field," *Plasma Phys. Contr. Fusion*, **27**, 1307 (1985).

6. T. SHIMADA, Y. HIRANO, Y. YAGI, A. A. NEWTON, and K. OGAWA, "Results from the Reversed Field Pinch Experiment on TPE-1RM15 with a Programmed Vertical Field," *Proc. 12th Conf. Plasma Physics and Controlled Fusion Research*, Nice, France, October 12–19, 1988, Vol. 2, p. 453, International Atomic Energy Agency (1988).

7. A. ALMAGRI, S. ASSADI, R. N. DEXTER, S. C. PRAGER, and J. C. SPROTT, "Studies of Large, Non-Circular, Reversed Field Pinch Discharges," *Nucl. Fusion*, **27**, 1795 (1987).

8. J. C. SPROTT, "Electrical Circuit Modeling of Reversed Field Pinches," *Phys. Fluids*, **31**, 2266 (1988).